

# Whole-transcriptome sequencing profiling identifies functional and prognostic signatures in patients with PTPRZ1-MET fusion-negative secondary glioblastoma multiforme

BAO-SHI CHEN<sup>1\*</sup>, KUAN-YU WANG<sup>2-4\*</sup>, SHU-QING YU<sup>1\*</sup>, CHUAN-BAO ZHANG<sup>1</sup>,  
GUAN-ZHANG LI<sup>4</sup>, ZHI-LIANG WANG<sup>4</sup> and ZHAO-SHI BAO<sup>1,3,4</sup>

Departments of <sup>1</sup>Neurosurgery and <sup>2</sup>Gamma Knife Center, Beijing Tiantan Hospital, Capital Medical University, Beijing 100050;  
<sup>3</sup>Center of Brain Tumor, Beijing Institute for Brain Disorders, Beijing 100069; <sup>4</sup>Department of Neurosurgery,  
Beijing Neurosurgical Institute, Capital Medical University, Beijing 100050, P.R. China

Received June 3, 2019; Accepted February 21, 2020

DOI: 10.3892/ol.2020.12049

**Abstract.** Gliomas are the most common type of primary brain tumor in adults with a high mortality rate. Low-grade gliomas progress to glioblastoma multiforme (GBM) in the majority of cases, forming secondary GBM (sGBM), followed by rapid fatal clinical outcomes. Protein tyrosine phosphatase receptor type Z1 (PTPRZ1)-MET proto-oncogene receptor tyrosine kinase (MET) (ZM) fusion has been identified as a biomarker for sGBM that is involved in glioma progression, but the mechanism of gliomagenesis and pathology of ZM-negative sGBM has remained to be fully elucidated. A whole-transcriptome signature is thus required to improve the outcome prediction for patients with sGBM without ZM fusion. In the present study, whole-transcriptome sequencing on 42 sGBM samples with or without ZM fusion from the Chinese Glioma Genome Atlas database identified mRNAs with differential

expression between patients with and without ZM fusion and the most significant survival-associated genes were identified. A 6-gene signature was identified as a novel prognostic model reflecting survival probability in patients with ZM-negative sGBM. Clinical characteristics in patients with a high or low risk score value were analyzed with the Kaplan-Meier method and a two-sided log-rank test. In addition, ZM-negative sGBM patients with a high risk score exhibited an increase in immune cells, NF- $\kappa$ B-induced pathway activation and a decrease in endothelial cells compared with those with a low risk score. The present study demonstrated the potential use of a next-generation sequencing-based cancer gene signature in patients with ZM-negative sGBM, indicating possible clinical therapeutic strategies for further treatment of such patients.

## Introduction

Gliomas are the most common type of neuroepithelial tumor of the central nervous system. Glioblastoma multiforme (GBM), referring to grade-IV glioma, is one of the deadliest of human cancer types. Based on the clinical course and molecular characteristics, GBMs may be classified into two subtypes (1-3). Primary GBMs refers to the vast majority of GBMs, which are thought to form *de novo* in the elderly, with a median overall survival of 15 months after maximal surgical resection, chemotherapy and radiotherapy (RT) (4). Secondary GBMs (sGBMs) typically progress from lower-grade tumors and affect younger patients. Since the Philadelphia chromosome was discovered in chronic myeloid leukemia in 1960, studies performed over the past six decades have identified fusion genes and proteins in a multitude of other types of cancer and through several different approaches (5). Fusion transcripts between fibroblast growth factor receptor 3 and transforming acidic coiled-coil containing protein 3 (6), and between the MYB proto-oncogene and the quaking homolog KH domain RNA binding protein were initially reported as the recurrent fusion transcripts in GBMs and pediatric gliomas, respectively (7). A previous study by our group identified a novel, recurrent fusion rearrangement involving the protein tyrosine phosphatase receptor type Z1 (PTPRZ1) and MET

*Correspondence to:* Dr Zhao-Shi Bao, Department of Neurosurgery, Beijing Tiantan Hospital, Capital Medical University, 119 South Fourth Ring Road West, Beijing 100050, P.R. China  
E-mail: baozhaoshi@bjtth.org

\*Contributed equally

**Abbreviations:** ZM-fusion, PTPRZ1-MET fusion; PTPRZ1, protein tyrosine phosphatase receptor type Z1; MET, MET proto-oncogene receptor tyrosine kinase; SIRPD, signal regulatory protein  $\delta$ ; ZNF117, zinc finger protein 117; KIF11, kinesin family member 11; FHDC1, FH2 domain containing 1; DDAH2, dimethylarginine dimethylaminohydrolase 2; C7orf60, base methyltransferase of 25S rRNA 2 homolog; IDH, isocitrate dehydrogenase; sGBM, secondary glioblastoma multiforme; CGGA, Chinese Glioma Genome Atlas; GO, Gene Ontology; GSEA, Gene Set Enrichment Analysis; ROC, receiver operating characteristic; AUC, area under the curve; HR, hazard ratio; PFS, progression-free survival; OS, overall survival

**Key words:** glioma, secondary glioblastoma multiforme, PTPRZ1-MET fusion, risk score, immune response

proto-oncogene receptor tyrosine kinase (MET) genes (ZM) in 15% of sGBMs (8). However, the mechanisms by which these genes contribute to gliomagenesis and progression in ZM-negative sGBM have remained to be fully elucidated.

In the present study, RNA sequencing was performed on 42 sGBM samples with or without ZM fusion. mRNAs with differentially expressed genes between patients with and without ZM fusion were identified and data were analyzed using a univariate Cox regression model in R language. A total of six mRNAs were selected to develop the risk score with random repeated sampling. ZM-negative patients with high risk scores had a relatively shorter overall survival (OS) time compared with those with low risk scores. The risk score was independent of clinical observations, including sex, age, isocitrate dehydrogenase (IDH) mutation status, O-6-methylguanine-DNA methyltransferase (MGMT) methylation status and therapeutic strategies. The prognostic value of the risk score on patients' OS was higher compared with the aforementioned clinical information. The immune cell response was enhanced in ZM-negative patients with high risk scores. Increased macrophages rather than endothelial score and NF- $\kappa$ B enrichment were identified in patients with high risk scores. In summary, the risk score signature may be robust in predicting the survival of patients with ZM-negative sGBM and may help identify novel therapeutic targets for further treatment for patients with ZM-negative sGBM.

## Materials and methods

**Samples.** In the present study, 42 tumor samples of confirmed sGBM were selected for the analysis. The samples were collected from January 2005 through to December 2018. The methods of the RNA sequencing were provided in a previous study (9). Our data used in the study were original samples to be used to generate the dataset. The samples were collected at Beijing Tiantan Hospital (Beijing, China) by our group and the RNA sequencing data were uploaded to the Chinese Glioma Genome Atlas (CGGA) RNA sequencing dataset (<http://www.cgga.org.cn>). For each patient, the following clinical information was collected: Sex, age, IDH status, MGMT promoter methylation status, RT, temozolomide (TMZ) chemotherapy and OS. Among the 42 cases, 35 were ZM fusion-negative, whereas the other 7 cases were ZM fusion-positive. Among the patients, 24 were male and 11 were female. The average age was 38.7 years (range, 8–58 years). The sample IDs of ZM fusion-negative samples are provided in supplementary Table SI. The clinical and molecular information of the 42 patients was obtained from the CGGA database and held in the medical records. The tumor tissues included in the CGGA database were obtained during surgery and informed consent was obtained from all patients.

**Gene selection.** Student's t-test was used to identify the differentially expressed genes between ZM-positive and -negative cases with  $P < 0.05$  used as a selection threshold. Univariate Cox regression was used to determine the genes associated with survival. The differentially expressed genes associated with survival were selected for further analysis. The hazard ratio (HR) of univariate Cox regression was used to develop the gene signature. The risk score model was developed

using the following formula: Risk Score =  $\sum_{i=1}^n \beta_i x_i$ , where  $\beta_i$  indicates the HR for each gene in the CGGA database of ZM fusion-negative cases and  $x_i$  indicates the expression value of each gene (10).

**Gene ontology (GO) analysis.** The correlation between the risk score and other genes was analyzed by Pearson correlation analysis using R programming language. The positively correlated genes ( $r > 0.4$ ;  $P < 0.05$ ) and the negatively correlated genes ( $r < -0.4$ ,  $P < 0.05$ ) were selected for analysis in the Database for Annotation, Visualization and Integrated Discovery (DAVID; <http://david.abcc.ncifcrf.gov/home.jsp>) to detect which functional terms were associated with the risk score (11).

**Gene set enrichment analysis (GSEA).** GSEA was used to analyze the association between the risk score and the hallmarks. The data were divided into two groups based on the risk score (low and high) and subjected to GSEA as previously described (12). The analysis was performed using the GSEA java software v4.0.3 (12).

**Statistical analysis.** In the present study, SPSS 16.0 (SPSS, Inc.), R software 3.2.5 (11) and GraphPad Prism 7.0 statistical software (GraphPad Software, Inc.) were used for data analysis and plotting. The R package 'survival' (<http://www.bioconductor.org/>) was used to analyze the most significant survival-associated mRNAs with the highest area under the curve (AUC) value in the dataset using the receiver operating characteristic curve analysis. The percentage of macrophages and endothelial cells was calculated by EPIC in R (13). Differentially expressed genes between ZM fusion-positive and -negative cases were determined by Student's t-test, which was also used to compare the risk scores between two groups. Survival analysis was performed using Kaplan-Meier survival analysis and univariate and multivariate Cox regression analysis. The analyzed factors included risk score, sex, age, IDH status, MGMT promoter methylation status, RT and TMZ chemotherapy.  $P < 0.05$  was considered to indicate statistical significance.

## Results

**Identification of survival-associated mRNAs.** To characterize the transcriptomic RNA expression in sGBMs, RNA was extracted from 42 sGBM specimens with or without ZM fusion to perform whole-transcriptome sequencing. Student's t-test was performed to identify differentially expressed genes between samples with and without ZM fusion (Fig. 1A). Univariate Cox regression was performed in the ZM-negative cohort and the genes associated with survival ( $P < 0.05$ ) were selected. The overlapping genes in the two analyses were selected for further analysis. Using the R package 'survival', the most significant survival-associated mRNAs with the highest AUC value in the dataset were identified (Fig. 1B), which yielded six genes: Signal regulatory protein  $\delta$  (SIRPD), kinesin family member 11 (KIF11), zinc finger protein 117 (ZNF117), base methyltransferase of 25S rRNA 2 homolog (C7orf60), FH2 domain containing 1 (FHDC1) and dimethyl-arginine dimethylaminohydrolase 2 (DDAH2). Each of these genes was differentially expressed between ZM-positive and

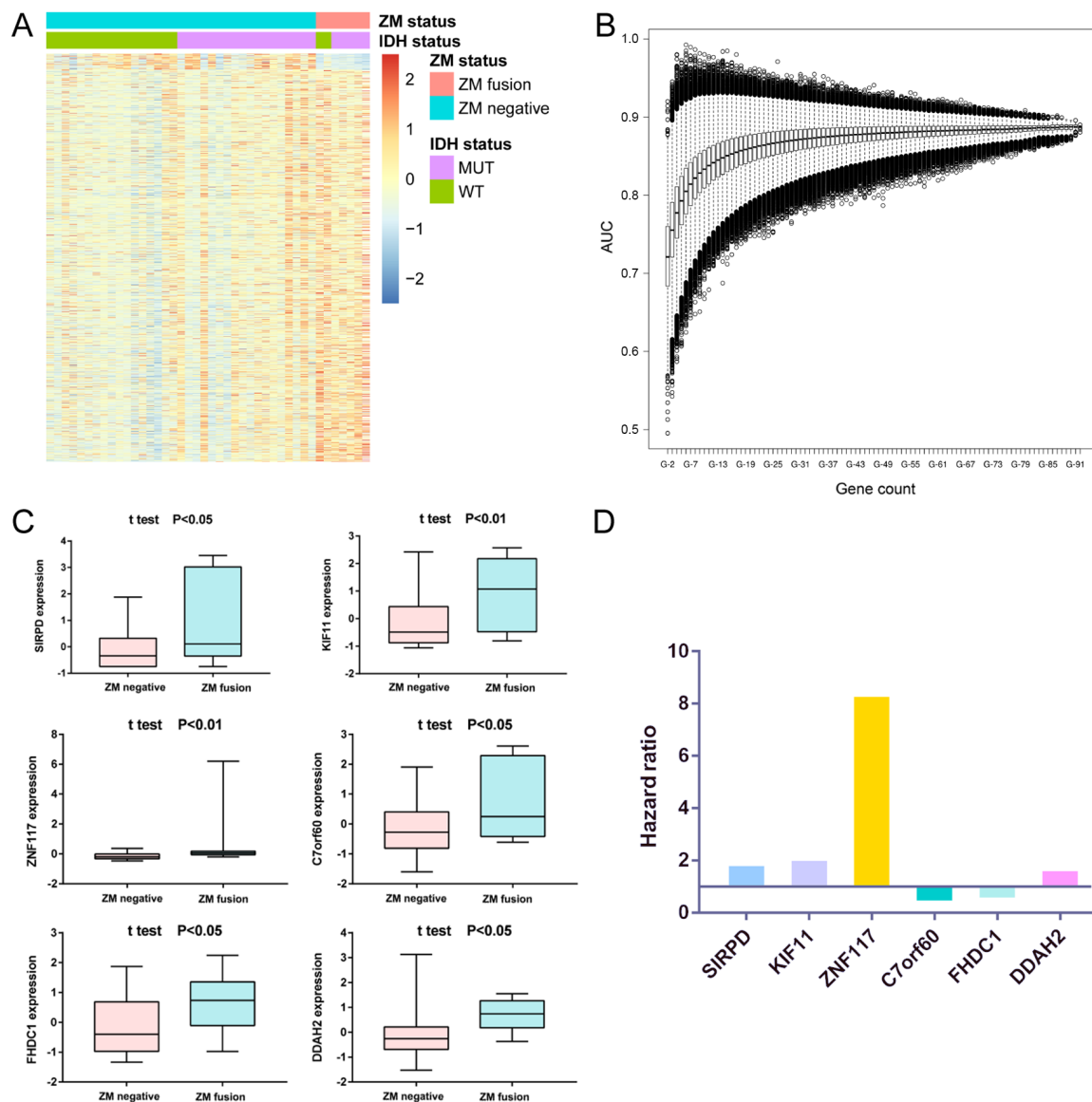


Figure 1. (A) Differentially expressed genes between ZM-positive and ZM-negative samples. (B) ROC curve analysis of different numbers of genes to select the risk score which predict the 1-year survival with the best prediction. The horizontal lines indicate the median AUC. The bars indicate the max and min AUC. The boxes indicated the 25-75% AUC. The circles represent the extreme value. (C) Expression of the six genes between ZM-positive and ZM-negative samples. The horizontal lines indicate the median expression. The bars indicate the maximum and minimum expression. The boxes indicated the 25-75% expression. (D) Hazard ratio of the six genes by univariate Cox regression analysis. ZM, protein tyrosine phosphatase receptor type Z1-MET proto-oncogene receptor tyrosine kinase fusion; AUC, area under the curve; IDH, isocitrate dehydrogenase; MUT, mutated; WT, wild-type; SIRPD, signal regulatory protein  $\delta$ ; KIF11, kinesin family member 11; ZNF117, zinc finger protein 117; C7orf60, base methyltransferase of 25S rRNA 2 homolog; FHDC1, FH2 domain containing 1; DDAH2, dimethylarginine dimethylaminohydrolase 2.

-negative tumor tissues and demonstrated lower expression levels in patients without ZM fusion (Fig. 1C). The HR of the survival analysis of each gene was also determined; the HRs of SIRPD, KIF11, ZNF117 and DDAH2 were positive, which indicated oncogenic characteristics in cell biological processes, whereas the HRs of C7orf60 and FHDC1 were negative, which indicated that these genes may suppress tumor occurrence (Fig. 1D).

**Clinical and genomic characteristics of risk score in patients with ZM-negative sGBM.** To investigate the clinical and genomic characteristics of the six selected genes, different weights were assigned to each gene for an independent risk score. The risk score of each patient was determined as

follows: Risk score =  $(0.5368 \times \text{SIRPD expression}) + (0.6481 \times \text{KIF11 expression}) + (2.1026 \times \text{ZNF117 expression}) + (-0.6095 \times \text{C7orf60 expression}) + (-0.4264 \times \text{FHDC1 expression}) + (0.4152 \times \text{DDAH2 expression})$ . The corresponding coefficients and P-values are presented in Table I. The high-risk score group was distinguished from the low-risk score group by the median score value as the cut-off value. Patients with ZM-negative sGBM with high risk scores exhibited poor prognosis, with significantly shorter OS times compared with those of patients with sGBM with low risk scores (median OS: High risk score, 233 days; low risk score, 572 days;  $P < 0.0001$ , log-rank test; Fig. 2A). In addition, the progression-free survival (PFS) time in the high- and low-risk groups was evaluated and patients with ZM-negative sGBM in the high-risk group demonstrated

Table I. HR (95% CI) and P-values generated from the univariate Cox regression analysis in the dataset for each gene.

Gene	HR	95% CI	P-value
SIRPD	1.711	1.025-2.855	0.040
KIF11	1.912	1.125-3.248	0.017
ZNF117	8.187	1.306-51.334	0.025
C7orf60	0.544	0.339-0.871	0.011
FHDC1	0.653	0.441-0.966	0.033
DDAH2	1.515	1.079-2.126	0.016

HR, hazard ratio; SIRPD, signal regulatory protein  $\delta$ ; KIF11, kinesin family member 11; ZNF117, zinc finger protein 117; C7orf60, base methyltransferase of 25S rRNA 2 homolog; FHDC1, FH2 domain containing 1; DDAH2, dimethylarginine dimethylaminohydrolase 2.

a significantly shorter PFS time compared with patients in the low-risk group, consistent with the trends of the OS time (Fig. 2B). The correlation between the risk score and mRNA expression was analyzed; the results indicated that the risk score may be a potential prognostic indicator (Fig. 2C).

*Clinical indications of risk score as an independent marker for prognosis.* The association between the risk score and clinical indicators, including sex, age, IDH status, MGMT promoter methylation status, RT and TMZ chemotherapy, was analyzed. The results demonstrated that the risk score was independent of sex, age, IDH mutation status, RT and TMZ chemotherapy, but associated with MGMT promoter methylation status (Fig. 3A). Uni- and multivariate Cox regression analysis was performed on these clinical factors. IDH status, risk score and TMZ chemotherapy were identified as potential prognostic markers by univariate Cox analysis (Fig. 3B). In the multivariate analysis, the risk score was the only factor identified as an independent prognostic marker in ZM-negative sGBMs (Table II). Therefore, the risk score was the most significant marker to indicate survival in patients with ZM-negative sGBM.

*Functional pathway annotation in patients with different risk scores.* To investigate the potential functional pathways activated in patients with high or low risk scores, GO analysis was performed on genes positively or negatively associated with the risk score. Genes enriched in 'immune response', 'inflammatory response', 'positive regulation of T-cell proliferation' and 'cell division' were significantly positively associated with the risk score in patients (Fig. 4A), whereas those enriched in relatively normal GO terms were negatively associated with the risk score in patients (Fig. 4B). To study the potential effect of immune cell differences in the present cohort, reference gene expression profiles of a major tumor-infiltrating immune cell type (macrophages) were established and expression profiles were derived from endothelial cells. The reference profiles were obtained as cell type averages from the single-cell RNA sequencing data of melanoma samples from Tirosh and colleagues (14). The reference cohort contained only samples

from primary tumors and non-lymphoid metastasis. The reference gene expression profiles from each of the immune and endothelial cells were used to predict the expression profile of bulk tumor and to evaluate their association with the risk score of patients with ZM-negative sGBM. The results demonstrated that patients with sGBM without ZM fusion and a high risk score exhibited a significantly higher macrophage signature expression compared with that of patients with a low risk score (Fig. 5B). By contrast, patients with a high risk score exhibited a lower endothelial cell signature expression compared with that in patients with a low risk score (Fig. 5A), indicating that these pathways may induce immune cells and suppress endothelial cells in patients with a high risk score. GSEA was performed with the risk score ranging from low to high; ZM-negative patients with higher risk scores tended to exhibit a higher inflammatory response and tumor necrosis factor (TNF)- $\alpha$  signaling activation by NF- $\kappa$ B (Fig. 5C and D). These results may provide further therapeutic strategies for patients with ZM-negative sGBM.

## Discussion

Based on whole-transcriptome sequencing on 42 sGBM samples from our own internal data, six genes were identified as an independent signature with the most significant survival-associated mRNAs and the best AUC in sGBMs without ZM fusion.

SIRPD is a member of a signal regulatory protein family involved in signal transduction and cell adhesion (15). No evidence has been confirmed in association with cancer initiation or progression.

The ZNF117 gene encodes a protein containing multiple C<sub>2</sub>H<sub>2</sub>-type zinc finger motifs. It has been demonstrated to participate in the maturation and differentiation of adipocytes and may control fat accumulation (16). The association between ZNF117 and human cancer requires further investigation.

KIF11, which is located on chromosome 22, encodes a kinesin-like motor protein that participates in chromosome positioning, centrosome separation and bipolar spindle formation during cell mitosis (17). Interactions between KIF11, MCF7 and phosphatase and tensin homolog regulate chromosome stability (18). KIF11 has been identified as a novel prognostic biomarker and a treatment target for various types of cancer, including lung squamous cell carcinoma, prostate cancer and chronic myeloid leukemia (19-22). In addition, previous studies demonstrated that KIF11 was an important regulator of activity in tumor stem cells of esophageal and colorectal cancer (23) and that upregulation of KIF11 was associated with high-grade astrocytoma (24). Targeting KIF11 also altered the cell fate and reduced glioma cell invasion (25). Thus, KIF11 may be a potential therapeutic target in glioma treatment.

The FHDC1 gene is located on human chromosome 4q31.3 (26) and encodes a protein product involved in the developmental stages of the mouse brain and the actin- and microtubule-dependent regulation of Golgi morphology of human cells (27). However, a limited number of studies have demonstrated an association between the FHDC1 gene and cancer development and progression. Further clinical studies on FHDC1-induced glioma initiation and progression require to be performed.

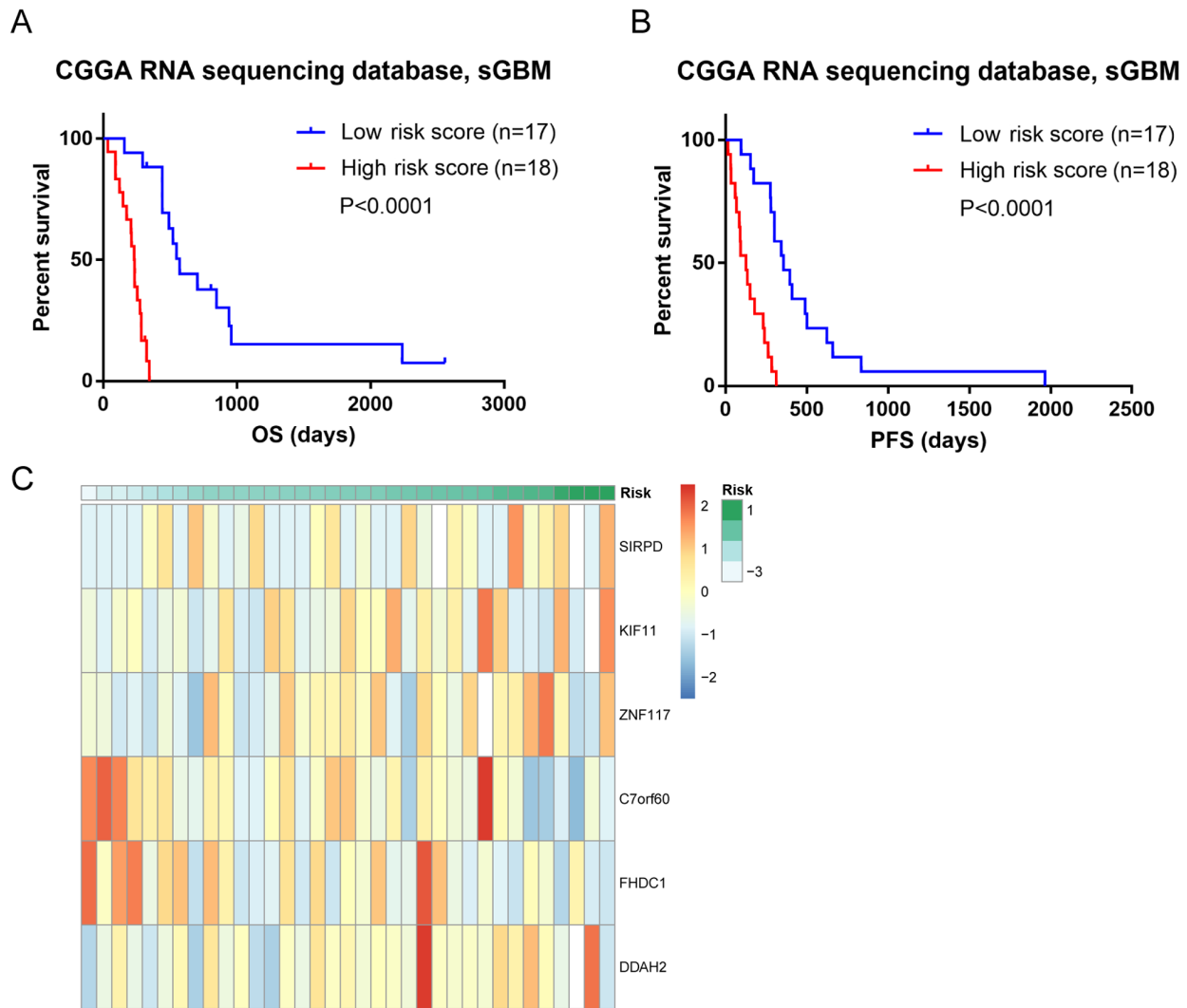


Figure 2. (A) Survival analysis of patients with ZM-negative sGBM in CGGA dataset. (B) PFS analysis in patients with ZM-negative sGBM in CGGA dataset. (C) The correlation between the risk score and the six gene expression. ZM, protein tyrosine phosphatase receptor type Z1-MET proto-oncogene receptor tyrosine kinase fusion; sGBM, secondary glioblastoma multiforme; CGGA, Chinese Glioma Genome Atlas; OS, overall survival; PFS, progression-free survival; SIRPD, signal regulatory protein  $\delta$ ; KIF11, kinesin family member 11; ZNF117, zinc finger protein 117; C7orf60, base methyltransferase of 25S rRNA 2 homolog; FHDC1, FH2 domain containing 1; DDAH2, dimethylarginine dimethylaminohydrolase 2.

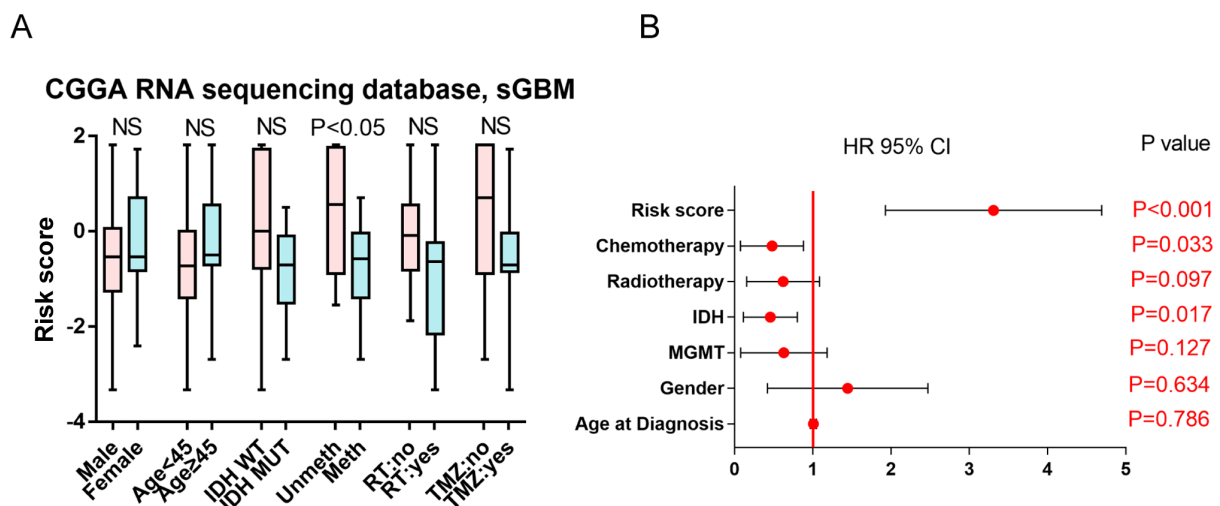


Figure 3. (A) Risk score associated with different clinical characteristics of patients. The horizontal lines indicate the median risk score. The bars indicate the maximum and minimum risk score. The boxes indicated the 25-75% risk score. (B) Forest plot of univariate Cox analysis. HR, hazard ratio; IDH, isocitrate dehydrogenase; MGMT, O-6-methylguanine-DNA methyltransferase; NS, no significance; MUT, mutated; WT, wild-type; unmeth, unmethylated MGMT promoter; CGGA, Chinese Glioma Genome Atlas; sGBM, secondary glioblastoma multiforme; RT, radiotherapy; TMZ, temozolomide.

Table II. Univariate and multivariate analysis of clinical prognostic parameters of patients with protein tyrosine phosphatase receptor type Z1-MET proto-oncogene receptor tyrosine kinase fusion secondary glioblastoma multiforme in the Chinese Glioma Genome Atlas RNA sequencing database.

Variable	Univariate analysis			Multivariate analysis		
	HR	95% CI	P-value	HR	95% CI	P-value
Age at diagnosis	1.006	0.966-1.047	0.786			
Sex	1.203	0.563-2.569	0.634			
MGMT	0.468	0.176-1.243	0.127			
IDH	0.369	0.163-0.836	0.017	1.087	0.392-3.018	0.392
Radiotherapy	0.503	0.223-1.133	0.097			
Chemotherapy	0.364	0.144-0.924	0.033	0.369	0.114-1.194	0.096
Risk score	3.116	2.032-4.777	<0.001	3.354	1.966-5.721	<0.001

All variables were considered as continuous variables. HR>1 indicates an increased risk, while HR<1 indicates a protective effect. HR, hazard ratio; IDH, isocitrate dehydrogenase; MGMT, O-6-methylguanine-DNA methyltransferase.

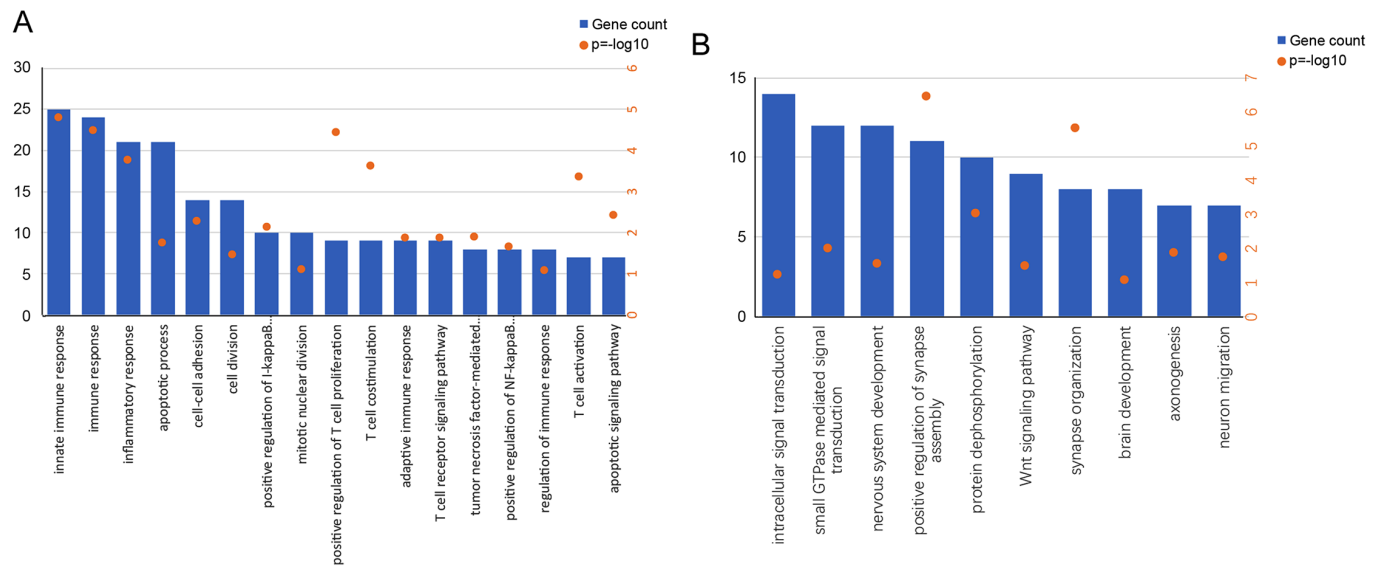


Figure 4. (A) Genes positively-associated with the risk score analyzed by Gene Ontology analysis in protein tyrosine phosphatase receptor type Z1-MET proto-oncogene receptor tyrosine kinase fusion-negative secondary glioblastoma multiforme. (B) Genes negatively-associated with the risk score analyzed by Gene Ontology analysis in ZM fusion-negative secondary glioblastoma multiforme.

DDAH2 encodes a dimethylarginine dimethylaminohydrolyase, which is important in nitric oxide generation by regulating the cellular concentrations of methylarginines. DDAH2 has been demonstrated to be associated with various types of disease, including hypertension (28), type 2 diabetes (29) and cancer. Upregulation of DDAH2 is associated with the invasiveness of lung adenocarcinoma by inducing proliferation and capillary-like tube formation of vascular endothelial cells (30). Further studies may focus on the therapeutic applications and the tumorigenic mechanisms of DDAH2 in other types of human cancer.

C7orf60, also known as the base methyltransferase of 25S rRNA 2 homolog gene, was identified as a genomic event in human complementary DNA (31,32) and associated with smoking cessation (33) and *Saccharomyces cerevisiae* infection (34). However, C7orf60 has not been demonstrated to be associated with cancer initiation or development.

In the present study, these six genes were assigned as an independent signature with the most significant survival-associated mRNAs and the best AUC. Patients with ZM-negative sGBM and a high risk score exhibited a shorter OS and PFS compared with those with a low risk score, revealing prog-



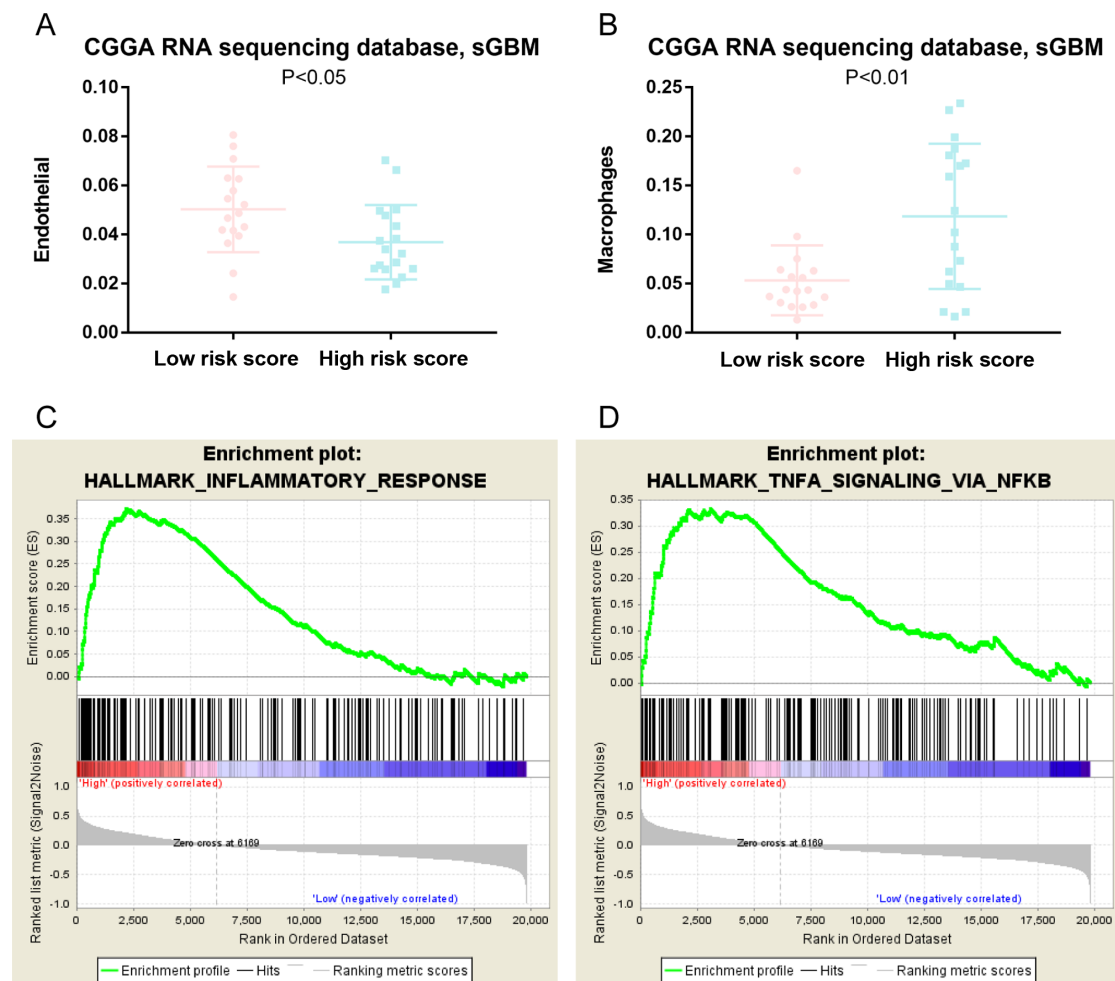


Figure 5. (A) Endothelial cell signature expression between patients with a low and high risk score. (B) Macrophage signature expression between patients with a low and high risk score. (C and D) Gene set enrichment analysis of the risk score in protein tyrosine phosphatase receptor type Z1-MET proto-oncogene receptor tyrosine kinase fusion-negative sGBM. TNF, tumor necrosis factor; sGBM, secondary glioblastoma multiforme; CGGA, Chinese Glioma Genome Atlas.

nostic value independent of other clinical features, including age, gender, IDH mutation and MGMT promoter methylation status.

Over the past decades, the tumor microenvironment and a number of tumor-associated cell types, including endothelial cells, pericytes, immune inflammatory cells, cancer-associated fibroblasts and stem and progenitor cells of the tumor stroma, have increasingly been demonstrated to contribute to the biology of numerous tumors and to regulate signaling that controls their development and progression. Immune cells differ in their gene expression profiles depending on their state and site of origin (for example blood or tumors) (35). Tumor-associated endothelial cell phenotypes have been implicated in cancer development and tumor-associated angiogenesis (36-38). These endothelial cells participate in establishing lymphatic vessels (39) that serve as channels for the seeding of metastases commonly observed in a number of cancer types. Tumor-promoting inflammatory cells include various macrophage subtypes that serve diverse and crucial roles in giving rise to tumorigenesis and malignancy (40). Qian and Pollard (41) demonstrated that tumor-associated macrophages suppressed cytotoxic T-cell and natural killer cell activity, which have been independently identified as myeloid-derived suppressor cells.

The results of the present study demonstrated that ZM-negative sGBM patients with a high risk score exhibited significantly higher macrophage expression compared with that of patients with a low risk score, whereas patients with a high risk score exhibited a lower endothelial cell signature expression compared with those with a low risk score, indicating increased immune cells and suppressed endothelial cells in samples from patients with a high risk score. In addition, NF- $\kappa$ B-induced TNF- $\alpha$  signaling activation tended to be enriched in patients with a high risk score, implying potential therapeutic targets for treatment in these patients.

The major advantage of the present study was the use of next-generation sequencing and systematic analysis under multidimensional conditions. The results identified a risk score that was associated with immune response in patients with ZM-negative sGBM and may guide further clinical management. However, the extent of the immune response and the type of macrophage activation that may promote glioma progression in ZM-negative sGBM still requires to be clarified. The cellular components within the tumor microenvironment requires to be studied further to reveal their clinical implications. In addition to the requirement for exploration of the immunoregulatory role of glioma cells, the results of the present study require validation in independent cohorts. Another limitation of the

present study is the relatively low number of sGBM samples and future studies may be performed in other, larger datasets, including The Cancer Genome Atlas.

In conclusion, the present study demonstrated the clinical utility of next-generation sequencing-based cancer gene profiling in sGBM. The results revealed the diagnostic value of a six gene-based risk score signature and clinical features of patients with ZM-negative sGBM. An increase in immune cells and a decrease in endothelial cells were identified in patients with a high risk score; potential therapeutic strategies were identified as NF- $\kappa$ B-induced TNF- $\alpha$  signaling activation in patients with ZM-negative sGBM with a high risk score.

## Acknowledgements

Not applicable.

## Funding

The present study was funded by the National Natural Science Foundation of China (grant no. 81502606), Beijing Municipal Administration of Hospitals' Youth Program (grant no. QML20160502), General Technological Program of Peking Education Commission (grant no. KM201810025023) and Beijing Nova Program (grant no. Z171100001117022).

## Authors' contributions

BC and KW designed the study and drafted the manuscript. SY revised the manuscript. SY, CZ, GL and ZW performed the data analyses. ZB contributed to the conception of the study and drafted the manuscript. All authors read and approved the final manuscript.

## Ethics approval and consent to participate

The present study was approved by the Beijing Tiantan Hospital institutional review board (Beijing, China) and informed consent was obtained from all individual participants included in this study.

## Patient consent for publication

Not applicable.

## Competing interests

The authors declare that they have no competing interests.

## References

- Wang Y and Jiang T: Understanding high grade glioma: Molecular mechanism, therapy and comprehensive management. *Cancer Lett* 331: 139-146, 2013.
- Louis DN, Ohgaki H, Wiestler OD, Cavenee WK, Burger PC, Jouvet A, Scheithauer BW and Kleihues P: The 2007 WHO classification of tumours of the central nervous system. *Acta Neuropathol* 114: 97-109, 2007.
- Louis DN, Perry A, Reifenberger G, von Deimling A, Figarella-Branger D, Cavenee WK, Ohgaki H, Wiestler OD, Kleihues P and Ellison DW: The 2016 World Health organization classification of tumors of the central nervous system: A summary. *Acta Neuropathol* 131: 803-820, 2016.
- Stupp R, Mason WP, van den Bent MJ, Weller M, Fisher B, Taphoorn MJ, Belanger K, Brandes AA, Marosi C, Bogdahn U, *et al*: Radiotherapy plus concomitant and adjuvant temozolomide for glioblastoma. *N Engl J Med* 352: 987-996, 2005.
- Mertens F, Johansson B, Fioretos T and Mitelman F: The emerging complexity of gene fusions in cancer. *Nat Rev Cancer* 15: 371-381, 2015.
- Singh D, Chan JM, Zoppoli P, Niola F, Sullivan R, Castano A, Liu EM, Reichel J, Porra P, Pellegatta S, *et al*: Transforming fusions of FGFR and TACC genes in human glioblastoma. *Science* 337: 1231-1235, 2012.
- Bandopadhyay P, Ramkissoon LA, Jain P, Berghthold G, Wala J, Zeid R, Schumacher SE, Urbanski L, O'Rourke R, Gibson WJ, *et al*: MYB-QKI rearrangements in angiocentric glioma drive tumorigenicity through a tripartite mechanism. *Nat Genet* 48: 273-282, 2016.
- Bao ZS, Chen HM, Yang MY, Zhang CB, Yu K, Ye WL, Hu BQ, Yan W, Zhang W, Akers J, *et al*: RNA-seq of 272 gliomas revealed a novel, recurrent PTPRZ1-MET fusion transcript in secondary glioblastomas. *Genome Res* 24: 1765-1773, 2014.
- Zhang C, Cheng W, Ren X, Wang Z, Liu X, Li G, Han S, Jiang T and Wu A: Tumor Purity as an Underlying Key Factor in Glioma. *Clin Cancer Res* 23: 6279-6291, 2017.
- Chai R, Zhang K, Wang K, Li G, Huang R, Zhao Z, Liu Y and Chen J: A novel gene signature based on five glioblastoma stem-like cell relevant genes predicts the survival of primary glioblastoma. *J Cancer Res Clin Oncol* 144: 439-447, 2018.
- Wang Z, Zhang C, Liu X, Wang Z, Sun L, Li G, Liang J, Hu H, Liu Y, Zhang W and Jiang T: Molecular and clinical characterization of PD-L1 expression at transcriptional level via 976 samples of brain glioma. *Oncoimmunology* 5: e1196310, 2016.
- Wang K, Huang R, Li G, Zeng F, Zhao Z, Liu Y, Hu H and Jiang T: CKAP2 expression is associated with glioma tumor growth and acts as a prognostic factor in high-grade glioma. *Oncol Rep* 40: 2036-2046, 2018.
- Pogorelyy MV, Fedorova AD, McLaren JE, Ladell K, Bagaev DV, Eliseev AV, Mikelov AI, Koneva AE, Zvyagin IV, Price DA, *et al*: Exploring the pre-immune landscape of antigen-specific T cells. *Genome Med* 10: 68, 2018.
- Tirosh I, Izar B, Prakadan SM, Wadsworth MH II, Treacy D, Trombetta JJ, Rotem A, Rodman C, Lian C, Murphy G, *et al*: Dissecting the multicellular ecosystem of metastatic melanoma by single-cell RNA-seq. *Science* 352: 189-196, 2016.
- Deloukas P, Matthews LH, Ashurst J, Burton J, Gilbert JG, Jones M, Stavrides G, Almeida JP, Babbage AK, Bagguley CL, *et al*: The DNA sequence and comparative analysis of human chromosome 20. *Nature* 414: 865-871, 2001.
- Ambele MA, Dessels C, Durandt C and Pepper MS: Genome-wide analysis of gene expression during adipogenesis in human adipose-derived stromal cells reveals novel patterns of gene expression during adipocyte differentiation. *Stem Cell Res* 16: 725-734, 2016.
- van Ree JH, Nam HJ, Jeganathan KB, Kanakkanthara A and van Deursen JM: Pten regulates spindle pole movement through Dlg1-mediated recruitment of Eg5 to centrosomes. *Nat Cell Biol* 18: 814-821, 2016.
- Feizabadi MS, Jun Y and Reddy JN: Distinctions between dynamic characteristics of the single EG5 motor protein along neural vs. Cancerous microtubules. *Biochem Biophys Res Commun* 478: 1630-1633, 2016.
- Lu M, Zhu H, Wang X, Zhang D, Xiong L, Xu L and You Y: The prognostic role of Eg5 expression in laryngeal squamous cell carcinoma. *Pathology* 48: 214-218, 2016.
- Yin Y, Sun H, Xu J, Xiao F, Wang H, Yang Y, Ren H, Wu CT, Gao C and Wang L: Kinesin spindle protein inhibitor SB743921 induces mitotic arrest and apoptosis and overcomes imatinib resistance of chronic myeloid leukemia cells. *Leuk Lymphoma* 56: 1813-1820, 2015.
- Wissing MD, De Morree ES, Dezentje VO, Buijs JT, De Krijger RR, Smit VT, Van Weerden WM, Gelderblom H and van der Pluijm G: Nuclear Eg5 (kinesin spindle protein) expression predicts docetaxel response and prostate cancer aggressiveness. *Oncotarget* 5: 7357-7367, 2014.
- Martens-de Kemp SR, Nagel R, Stigter-van Walsum M, van der Meulen IH, van Beusechem VW, Braakhuis BJ and Brakenhoff RH: Functional genetic screens identify genes essential for tumor cell survival in head and neck and lung cancer. *Clin Cancer Res* 19: 1994-2003, 2013.



23. Imai T, Oue N, Sentani K, Sakamoto N, Uraoka N, Egi H, Hinoi T, Ohdan H, Yoshida K and Yasui W: KIF11 Is Required for Spheroid Formation by Oesophageal and Colorectal Cancer Cells. *Anticancer Res* 37: 47-55, 2017.
24. Liu L, Liu X, Mare M, Dumont AS, Zhang H, Yan D and Xiong Z: Overexpression of Eg5 correlates with high grade astrocytic neoplasm. *J Neurooncol* 126: 77-80, 2016.
25. Venere M, Horbinski C, Crish JF, Jin X, Vasanthi A, Major J, Burrows AC, Chang C, Prokop J, Wu Q, *et al*: The mitotic kinesin KIF11 is a driver of invasion, proliferation, and self-renewal in glioblastoma. *Sci Transl Med* 7: 304ra143, 2015.
26. Katoh M and Katoh M: Identification and characterization of human FHDC1, mouse Fhdcl and zebrafish fhdc1 genes in silico. *Int J Mol Med* 13: 929-934, 2004.
27. Copeland SJ, Thurston SF and Copeland JW: Actin- and microtubule-dependent regulation of Golgi morphology by FHDC1. *Mol Biol Cell* 27: 260-276, 2016.
28. Wang Z, Chen S, Zhang L, Lu G, Zhou C, Wang DW, Wang L, Badengmu B, Zhai Z and Qin L: Association between variation in the genes DDAH1 and DDAH2 and hypertension among Uyghur, Kazakh and Han ethnic groups in China. *Sao Paulo Med J* 134: 205-210, 2016.
29. Yuan Q, Hu CP, Gong ZC, Bai YP, Liu SY, Li YJ and Jiang JL: Accelerated onset of senescence of endothelial progenitor cells in patients with type 2 diabetes mellitus: Role of dimethylarginine dimethylaminohydrolase 2 and asymmetric dimethylarginine. *Biochem Biophys Res Commun* 458: 869-876, 2015.
30. Shiozawa T, Iyama S, Toshima S, Sakata A, Usui S, Minami Y, Sato Y, Hizawa N and Noguchi M: Dimethylarginine dimethylaminohydrolase 2 promotes tumor angiogenesis in lung adenocarcinoma. *Virchows Arch* 468: 179-190, 2016.
31. Kimura K, Wakamatsu A, Suzuki Y, Ota T, Nishikawa T, Yamashita R, Yamamoto J, Sekine M, Tsuritani K, Wakaguri H, *et al*: Diversification of transcriptional modulation: Large-scale identification and characterization of putative alternative promoters of human genes. *Genome Res* 16: 55-65, 2006.
32. Ota T, Suzuki Y, Nishikawa T, Otsuki T, Sugiyama T, Irie R, Wakamatsu A, Hayashi K, Sato H, Nagai K, *et al*: Complete sequencing and characterization of 21,243 full-length human cDNAs. *Nat Genet* 36: 40-45, 2004.
33. Rose JE, Behm FM, Drgon T, Johnson C and Uhl GR: Personalized smoking cessation: interactions between nicotine dose, dependence and quit-success genotype score. *Mol Med* 16: 247-253, 2010.
34. Sharma S, Watzinger P, Kotter P and Entian KD: Identification of a novel methyltransferase, Bmt2, responsible for the N-1-methyl-adenosine base modification of 25S rRNA in *Saccharomyces cerevisiae*. *Nucleic Acids Res* 41: 5428-5443, 2013.
35. Racle Y, de Jonge K, Baumgaertner P, Speiser DE and Gfeller D: Simultaneous enumeration of cancer and immune cell types from bulk tumor gene expression data. *Elife* 6: e26476, 2017.
36. Pasquale EB: Eph receptors and ephrins in cancer: Bidirectional signalling and beyond. *Nat Rev Cancer* 10: 165-180, 2010.
37. Ahmed Z and Bicknell R: Angiogenic signalling pathways. *Methods Mol Biol* 467: 3-24, 2009.
38. Dejana E, Orsenigo F, Molendini C, Baluk P and McDonald DM: Organization and signaling of endothelial cell-to-cell junctions in various regions of the blood and lymphatic vascular trees. *Cell Tissue Res* 335: 17-25, 2009.
39. Tammela T and Alitalo K: Lymphangiogenesis: Molecular mechanisms and future promise. *Cell* 140: 460-476, 2010.
40. Coffelt SB, Lewis CE, Naldini L, Brown JM, Ferrara N and De Palma M: Elusive identities and overlapping phenotypes of proangiogenic myeloid cells in tumors. *Am J Pathol* 176: 1564-1576, 2010.
41. Qian BZ and Pollard JW: Macrophage diversity enhances tumor progression and metastasis. *Cell* 141: 39-51, 2010.



This work is licensed under a Creative Commons Attribution-NonCommercial-NoDerivatives 4.0 International (CC BY-NC-ND 4.0) License.